

ROTATIONAL-LEVEL-DEPENDENT QUENCHING OF OH(A $^2\Sigma^+$) AT FLAME TEMPERATURES

Jay B. JEFFRIES, Katharina KOHSE-HÖINGHAUS¹, Gregory P. SMITH,
Richard A. COPELAND and David R. CROSLY

Chemical Physics Laboratory, SRI International, Menlo Park, CA 94025, USA

Received 27 June 1988; in final form 23 August 1988

The collisional quenching of OH(A $^2\Sigma^+$, $v'=0$) is studied by laser-induced fluorescence in the burnt gases of low-pressure (7 Torr) stoichiometric H₂/O₂/N₂O flames. The temperature of these flames is adjusted between 1200 and 2300 K by altering the O₂/N₂O mixing ratio. The variation of the quenching rate constant with rotational level in the OH(A) for H₂O collider is substantially less at 2300 K than previously observed at room temperature. The OH(A) quenching rate constant by atomic hydrogen at 1200 K is estimated $k=8\times 10^{-10}$ cm³ s⁻¹.

1. Introduction

A desire to understand the process of collisional quenching of the electronically excited A $^2\Sigma^+$ state of the OH molecule has motivated many studies in this laboratory and elsewhere. The fundamental and applied importance of OH justifies such a detailed examination. This radical is small enough to be amenable to modern theoretical calculation of realistic potential surfaces and trajectories. It is a crucial intermediate in the chemical kinetics of combustion and the atmosphere, where its detection via laser-induced fluorescence (LIF) requires knowledge of the fluorescence quantum yield for a wide variety of conditions.

Through LIF studies on OH, we have developed a consistent picture of collisional processes involving the A state. The cross sections σ_Q and σ_v for, respectively, quenching [1] of $v'=0$ and vibrational energy transfer [2,3] from $v'=1$ to $v'=0$ are large for many collisional partners, indicating the influence of long-range attractive forces and the formation of a collision complex. A decrease in all measured σ_Q with increasing temperature [4,5], i.e.

collision velocity, is strong support for this conclusion.

The dependence of both σ_v [2,3] and σ_Q [1,6,7] on rotational quantum number N' is particularly interesting. For some colliders, the cross sections at 300 K fall as much as a factor of two as N' increases from 0 to 5. This behavior has been attributed [1,2] to the anisotropic attractive interaction surface between the polar OH(A) and the collider species. In the quenching collision a non-rotating OH(A) approaches along valleys in the surface; however, as the OH(A) rotates, the effective anisotropy of the surface is washed out, and the pair cannot find these entrance channels as efficiently. (Recently, a significant rotational level dependence of σ_Q has also been observed for the A $^3\Pi_1$ state of NH in both flow cells [7] and flames [8], although the collision partner and temperature dependence [7-9] do not conform to an attractive forces picture like that used for OH.)

For LIF monitoring of OH, estimates of σ_Q for environments with a variety of colliders and temperatures are necessary. This has been considered for combustion applications [10], using a temperature dependence incorporating the attractive forces collision model [4] and the N' dependence observed at room temperature [1]. No well characterized experimental results are available at realistic flame temperatures, above 1400 K, to validate these ex-

¹ On leave from DFVLR, Institut für Physikalische Chemie der Verbrennung, D-7000 Stuttgart, Federal Republic of Germany.

trapolations. Furthermore, quenching only by stable molecular colliders is considered [10], even though there may be large concentrations of radicals, particularly hydrogen atoms, which could have large σ_Q .

In summary, we know that for OH the excited state collision dynamics are governed by an anisotropic attractive surface, resulting in a temperature (velocity) and rotational level dependence of the cross sections. A key remaining question is the temperature dependence of that rotational dependence. For flame applications, direct knowledge of that quenching at high temperature, as well as quenching by radicals is needed.

In the present study, we measure σ_Q for OH($A^2\Sigma^+$) in several flames at low pressure, and obtain results for both H₂O and H-atom colliders. We examine the collider H₂O at 2300 K in an H₂/N₂O flame and find that the N' dependence seen at room temperature [1,6,11] has disappeared. That result is consistent with our understanding of OH(A) quenching. H₂ flames having burnt gas temperatures ranging from 1200 to 2300 K are obtained using mixtures of O₂ and N₂O oxidants. The interpretation of results in terms of species-specific σ_Q requires a model of the flame chemistry. Applying such a model we conclude that hydrogen atoms quench OH(A) with a large cross section. This finding is both interesting for dynamics and significant for flame diagnostics.

2. Experiment

The apparatus, which has been described earlier [12], consists of a low-pressure burner, an excimer-laser-pumped dye laser and a fluorescence detection system. Stoichiometric mixtures of H₂ with either N₂O or O₂ or mixtures of both oxidizers are burned at 7.2 Torr on a 6 cm diameter flat-flame burner. The frequency-doubled radiation from sulfarhodamine-B dye excites different rotational transitions in the (0,0) band of the OH $A^2\Sigma^+ - X^2\Pi_1$ electronic system. Photodiodes monitor the laser power before and after its passage through the flame.

The fluorescence in the (0,0) band is collected and focused with $f/3$ and $f/4$ lenses, respectively, onto the entrance slit of a monochromator. The time-resolved fluorescence decays must be observed with a

broad bandwidth so that rotational energy transfer during the fluorescence decay does not affect the signal by a change in detection efficiency. This band-pass is produced by modification of the monochromator (0.3 m Jarrel-Ash) output slits. A 0.5 mm entrance slit and a 4 mm output slit provide a trapezoidal spectral response with a 20 nm top and a 23 nm base. This spectral response encompasses the entire (0,0) band of the OH $A-X$ system when centered at 312 nm [13]. The fluorescence signal is time-resolved with a 100 MHz transient digitizer.

The fluorescence time decay of the entire (0,0) band is measured after excitation of a specific rotational level N' in the $A^2\Sigma^+$. The burner is positioned so that the flame is probed at a height well above the reaction zone of the flame. Thus the measurements are made in a region of the burnt gases where the species concentrations are slowly varying. However, at the very low pressures of our flames, the equilibrium concentrations of the flame species are not necessarily reached, and a discussion of the chemistry model used to estimate the concentrations of the various collider species is presented later in the section on flame chemistry.

3. Results

An example of the time-resolved fluorescence signal after excitation of $N' = 8$ in a H₂/N₂O flame is presented in fig. 1. The logarithm of the data is linear for more than three decay constants which demonstrates that the decay is well characterized by a single exponential. The fluorescence decay lifetime is then given by

$$\tau_D = (A + Q)^{-1}, \quad (1)$$

where A is the radiative decay rate and Q is the total quenching rate,

$$Q = \sum k_{Qi} n_i, \quad (2)$$

where k_{Qi} is the rate constant for the collisional quenching of OH(A) by species i , n_i is the density of species i , and the sum is over all the species present at the point of measurement. We remove the variation in Q caused by the temperature dependence of the density by defining an effective removal rate constant $k_D \equiv Q/n$, where n is the total density

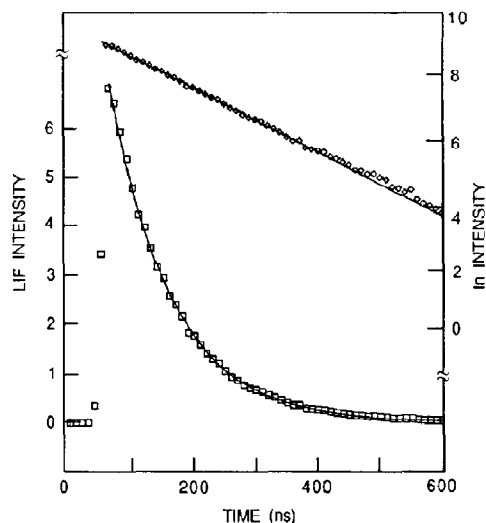


Fig. 1. Time-resolved LIF signal from OH($A^2\Sigma^+$) after excitation of $N' = 8$ in the burnt gases of a 7.2 Torr stoichiometric H_2/N_2O flame averaged over 500 laser shots. Data are points and smooth curve is fit to single exponential.

of the flame gas. To obtain n , we must measure the gas temperature and pressure.

The spatially resolved gas temperature in the flame is obtained from rotational excitation spectra in the OH A-X (0,0) band. The temperature measurements and the precautions required to ensure high accuracy of the results are presented in detail in ref. [13]. Fig. 2 shows the measured temperature versus height above the burner for the stoichiometric H_2/N_2O and H_2/O_2 flames. The large difference in temperature between the flames burning in O_2 and N_2O is striking in view of their very similar adiabatic flame temperatures. The low temperature of low-pressure H_2/O_2 flames has been observed before [14], and is a direct result of the reduced $H + O_2$ chain branching and reduced recombination at low pressure. We use this difference to "tune" the flame temperature over the range 1200–2300 K by adjusting the mixing ratio of O_2 and N_2O . Temperature profiles [13] are measured for each of the mixed oxidizer flames, ($2N_2O/O_2$) = 0.66, 1.0, 1.33, 1.67, and 2.0. As expected, the shapes of all these profiles exhibit a smooth transition between the two limiting cases, shown in fig. 2, pure O_2 and pure N_2O .

The fluorescence decay lifetime is measured after exciting $N' = 3, 8$, and 16 of the OH(A) in all six

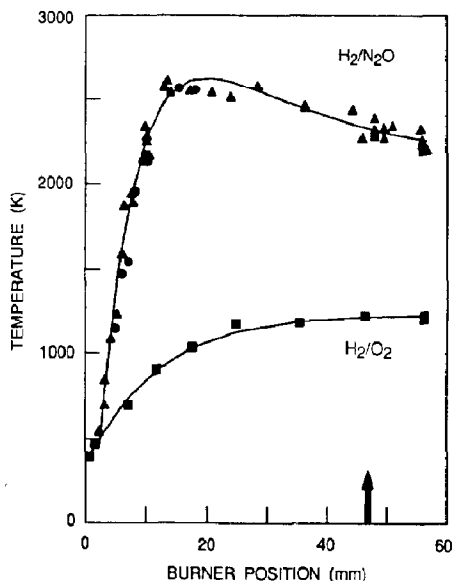


Fig. 2. OH rotational excitation scan measurements of temperature for the 7.2 Torr stoichiometric H_2/N_2O (triangles) and H_2/O_2 (boxes) flames versus height above the burner. Solid circles are rotational temperature measurements on NH. The arrow at 46 mm denotes that point in the flame where quenching measurements are made.

flames at a position in the flame 46 mm above the burner. The radiative lifetime (slightly different for the three excited levels [15]) is then subtracted and the resulting rate divided by the density to obtain the effective removal rate constant. Fig. 3 displays the results as a function of temperature in the six dif-

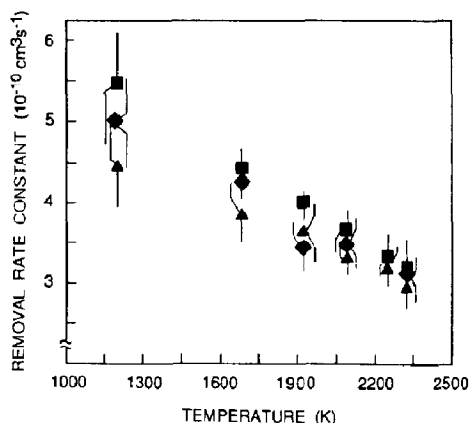


Fig. 3. Effective removal rate constants for OH(A) $N' = 3$ (boxes), $N' = 8$ (diamonds), and $N' = 16$ (triangles) versus temperature in stoichiometric H_2 flames at 7.2 Torr with mixtures of O_2 and N_2O oxidant. Error bars are 2σ .

ferent flames. Each measurement is made 5–30 times, and the error limits are the 2σ statistical errors about the mean of these measurements. The results in fig. 3 suggest a small systematic dependence of the removal rate constant on the rotational level initially excited; this dependence diminishes with increasing temperature.

The variation of k_D with rotational level becomes evident when we consider the ratio $k_D(N'=3)/k_D(N'=16)$ as a function of temperature. For this ratio, any uncertainty in k_D from the temperature and pressure measurements cancel if τ_D is measured for both rotational levels for an identical flame. Taking repeated measurements on a given flame and calculating only the statistical precision we find the ratio $k_D(3)/k_D(16)$ declines from 1.20 ± 0.06 at 1200 K to 1.02 ± 0.04 at 2300 K.

The interpretation of the observed dependence of the removal rate constant on rotational level requires a measure of the amount of rotational energy transfer during the fluorescence lifetime of the OH(A). Complete rotational relaxation to a thermal distribution in the excited $A^2\Sigma^+$ state is not observed in either atmospheric-pressure [16] or low-pressure [17] flames. We measure the rotational distribution by wavelength-resolved LIF spectra after tuning the laser to excite one of the rotational levels, $N' = 3, 8,$ or 16 . These spectra for the H_2/N_2O flame are shown in fig. 4. The fluorescence is resolved with 0.15 nm (fwhm) resolution, and the signal is integrated by a boxcar integrator with the time gate adjusted to equal two decay constants. The integration period is chosen to match with the single exponential fit over the range from 90% to 10% of the signal intensity used in evaluation of k_D .

Each of the initially excited N' in fig. 4 have distinctly different rotational distributions, which we characterize as low- N' , mid- N' , and high- N' distribution. For $N' = 3$, 33% of the fluorescence originates from the initial level, for $N' = 8$, 36%, and for $N' = 16$, 38%; values which all agree within their precision. The spectra for the other flames are surprisingly similar and show no noticeable differences with those in fig. 4. For example, in the H_2/O_2 flame with $N' = 8$, 38% of the fluorescence originates from the initial level. Thus, the measured rotational distributions show that the rotational population is largest in the directly excited level, and that the wide-band

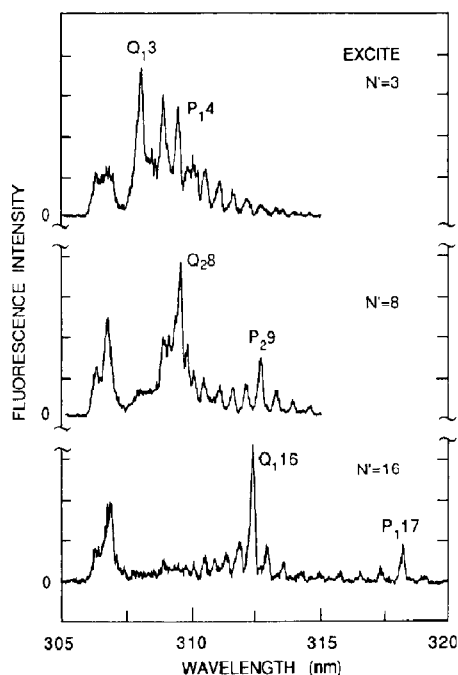


Fig. 4. OH LIF spectra in the burnt gases of a 7.2 Torr stoichiometric H_2/N_2O flame after initially exciting $N' = 3, 8,$ or 16 , using boxcar integration of the signal for two fluorescence lifetimes.

detection samples only fluorescence from a limited number of levels peaking around the directly excited level.

We obtain additional evidence on how much the rotational-level-dependent quenching in fig. 3 might be diminished by rotational energy transfer. The data in fig. 3 are obtained from fits to a single exponential from 90% to 10% of the fluorescence intensity. This corresponds to a time interval of ≈ 2 decay constants during which rotational transfer can occur. If the data instead are fit to an interval 90–30%, ≈ 1 decay constant, there is less time for rotational transfer. When the shorter time interval is fit, we observe only minor changes in the decay constants. For example in the H_2/O_2 flame at 1200 K where the rotational dependence is the largest, the ratio $k_D(3)/k_D(16)$ changes from 1.20 ± 0.06 to 1.17 ± 0.10 with the smaller fitting interval, and in the H_2/N_2O flame at 2300 K the ratio changes from 1.02 ± 0.04 to 1.06 ± 0.06 . These observations indicate that rotational energy transfer is not responsible for the lack of rotational level dependence of k_D observed at 2300 K.

4. Flame chemistry model

In order to get the H and H₂O mole fractions, we estimate the gas composition from the predictions of a chemical kinetic model which uses our measured temperature profile as input data. We then compare measured OH concentrations with the predicted ones as an indicator of the reliability of the prediction. Note that we make our quenching measurements in the burnt gases where concentrations and temperatures are changing much more slowly than in the reaction zone.

The flame model calculations are performed using the flame code PREFLAME [18] incorporating the detailed chemistry package CHEMKIN [19] with our own reaction mechanism [20]. The rate coefficients for the H₂/O₂ system are taken from Warnatz [21]. For the H₂/N₂O system the recommendations of Hanson and Salimian [22] are used, except for the reaction of H with N₂O, which forms the OH or NH radical [23]. We estimate the rate constants for the reactions of NH with other radicals. Under our conditions the minor species H₂O₂, HNO, and NH₂ do not influence the concentrations of any species with concentration above 100 ppm, and thus are omitted in the mechanism. The burner surface temperature is assumed to be 370 K, a value inferred from the lowest measured temperature at 0.6 mm above the burner surface in the H₂/O₂ flame. This assumed surface temperature has no significant influence on the calculated species in the burnt gas region of the flame.

The results of the model calculations are compared to the measured OH concentration profiles. The concentration measurements and related accuracy considerations are discussed elsewhere [24]. The shape of the predicted [OH] versus height above the burner, including the crucial [OH] rise, is in each flame well represented by the model simulation. For the H₂/N₂O flame, an absorption measurement is used to provide an absolute [OH] scale; the measured and calculated [OH] agreed to within the 30% error limits of the absorption experiment.

Fig. 5 shows the gas composition and temperature as a function of the fraction oxidized by O₂; the concentration values for the six flames are connected by smooth curves. The mole fraction of water, the expected dominant quencher [10], remains almost

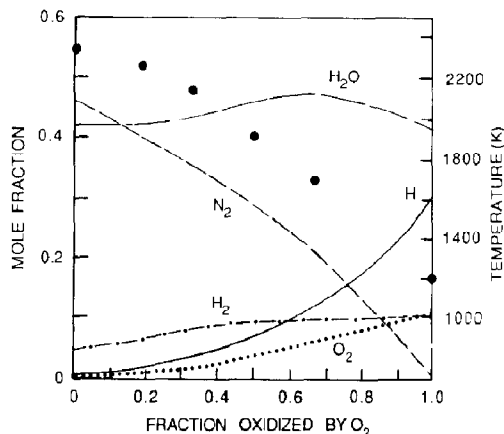


Fig. 5. Points are the measured temperatures of the six stoichiometric H₂ flames with mixtures of O₂ and N₂O oxidant at a burner height of 46 mm. Lines are the model calculations of mole fractions of N₂ (short dashes), H₂O (long dashes), H atoms (solid line), H₂ (dash-dotted line), and O₂ (dotted line) at the same point in the burnt gases of flames studied versus the fraction of the fuel oxidized by O₂.

constant for all flames. As the oxidizer is shifted from N₂O to O₂ the amount of N₂ formed correspondingly decreases. Note the high concentration of H atoms at the low temperatures. The fraction of stable molecules, other than H₂O and N₂, is predominately unburnt H₂ and O₂ in the flames with high O₂ content and mainly NO and H₂ in the flames with large N₂O mole fraction. Several minor constituents are not plotted in fig. 5. The concentration of NO is not present in the H₂/O₂ flame and rises to 4% in the H₂/N₂O flame; other radicals, O and OH, vary from 2% to 5%.

The uncertainty in the species concentrations predicted by the model is difficult to assess. We measure the quenching in the burnt gases to avoid spatial gradients in the species concentrations. We gain confidence in the model by the agreement between predicted and measured [OH]. The only significant (> 10%) difference between the model and equilibrium concentrations is the large [H] in the H₂/O₂ flame. If we recalculate the H₂/O₂ flame with a 20% increase in the sensitive rate constants [21] for H+O₂ and OH+H₂ the [H] only declines by 5%. Variation in the input temperatures of 100 K show similar effects on the model results. Thus, we expect our species concentration estimates for [H₂O] and [H] are valid to ± 10%.

5. Discussion

The determination of quenching cross sections as a function of temperature for the major flame constituents from the removal rate constant data in fig. 3 is not without ambiguity, because of the simultaneous changes in the gas composition and the temperature in each of the flames. However, we can make three conclusions about the collision dynamics of the $\text{OH}(\text{A}^2\Sigma^+)$ electronic energy transfer and two conclusions useful for flame studies.

First, the thermally averaged quenching cross section of $\text{OH}(\text{A})$ by H_2O decreases between room temperature and 2300 K, a conclusion which supports an earlier measurements of $\sigma_Q = 26 \pm 3 \text{ \AA}^2$ at 1200 K [4]. In the H_2/O_2 flame in the burnt gases at 2300 K the major species H_2O and N_2 are more than 88% of the gas with the remainder H_2 , NO , and OH . Recalling the $< 0.6 \text{ \AA}^2$ cross section for $\text{OH}(\text{A})$ quenching by N_2 at 1200 K [5], we assume that N_2 quenching is negligible. Thus, more than 80% of the quenching in the $\text{H}_2/\text{N}_2\text{O}$ flame at 2300 K is due to water, which leads to a cross section of 25 \AA^2 . Clearly the cross section decreases between room temperature [1,6] and 2300 K.

Second, we conclude that the magnitude of the rotational level dependence for H_2O quenching of $\text{OH}(\text{A})$ diminishes with temperature between 300 and 2300 K. At room temperature there is disagreement on both the magnitude and sign of the rotational level dependence of the $\text{OH}(\text{A})$ quenching rate constant for H_2O . There are three studies [1,6,11] which find that the $\text{OH}(\text{A})$ quenching rate constant at 300 K declines with increasing N' , but there is another [25] which measures an increase in the quenching rate constant with N' . Our arguments here are based on the data in refs. [1,6,11]. At room temperature, the quenching rate constant of $\text{OH}(\text{A})$ with H_2O decreases $\approx 15\%$ for [1] $0 \leq N' \leq 7$ and $\approx 40\%$ for [6] $3 \leq N' \leq 16$. This corresponds to a ratio $k_D(3)/k_D(16) = 1.7$. The data at 2300 K in fig. 3 show less than a 6% variation between a low- N' distribution peaked on $N' = 3$ and a high- N' distribution peaked on $N' = 16$. Since we have concluded that at least 88% of the quenching in the flame at 2300 K is due to water collisions, the rotational level variation of the quenching of $\text{OH}(\text{A})$ by H_2O decreases over the range 300–2300 K.

Fig. 3 also suggests a systematic decrease in the total variation of removal rate constant with rotational level as the temperature increases from 1200 to 2300 K; recall that $k_D(3)/k_D(16)$ declines from 1.2 to 1.02. This decrease may reflect the temperature dependence of the rotational level dependence or it may be a result of the changing species composition in the flames. However, if the latter is true and the rotational level dependence seen in the 1200 K flame is due to colliders other than H_2O , then the rotational level dependence of the $\text{OH}(\text{A})$ quenching with H_2O must disappear over an even smaller temperature range, 300–1200 K.

This decrease in the rotational level dependence of the quenching is consistent with our hypothesis about the collision dynamics. For $\text{OH}(\text{A})$ in low rotational levels and at low collision velocity, attractive valleys in the potential surface should enhance the complex formation which leads to quenching. Such enhancement would not occur for higher rotational levels which therefore have smaller σ_Q . Because the complex formation is governed by attractive forces, we expect σ_Q for both high and low levels to decrease with increasing temperature. However σ_Q for lower levels would decrease more, because the approach along the preferred directions on the surface are now inhibited by the faster collision velocity. This is in accord with the present experimental results.

The third conclusion from these data is an estimate of the cross section for $\text{OH}(\text{A})$ quenching by H atoms. In the 1200 K burnt gases of the H_2/O_2 flame the chemistry model predicts that $\approx 30\%$ of the gas composition is atomic hydrogen. At 1200 K quenching rate constants are available [4] for the other major species, H_2O , H_2 , and O_2 . Using the gas composition data in fig. 5, the measured rate constants for the other species [4], and the effective removal rate constant in fig. 3, we estimate the rate constant at 1200 K for $\text{OH}(\text{A})$ quenching by H atoms is $k_Q = 8 \times 10^{-10} \text{ cm}^3 \text{ s}^{-1}$. This gives a $\sigma(\text{H}) = 16 \pm 5 \text{ \AA}^2$, which is consistent with the combination of a physical picture of $\text{OH}(\text{A})$ quenching dominated by attractive forces and the room temperature measurement [26] of $\sigma(\text{OH}) = 22 \text{ \AA}^2$. The quenching rate from this cross section is augmented by the high velocity of the low mass hydrogen atoms.

Two important conclusions concerning flame studies are also observed. First, we note that these

low-pressure stoichiometric flames can be tuned in temperature over a large range, 1200–2300 K, simply by adjusting the O₂/N₂O mixing ratio. This discovery will allow many different flame studies to be conducted over a much wider range of temperatures than is possible with diluent addition. Second, in the 7.2 Torr H₂/O₂ flame, H atoms are responsible for > 50% of the quenching of OH(A) even well beyond the flame front, demonstrating the importance of radical–radical quenching under flame conditions, at least for these cool low-pressure flames.

Acknowledgement

The study was supported by Basic Energy Sciences Program of the Department of Energy. Computations were performed on the Chemical Physics Laboratory VAX 11/750 purchased by NSF Grant PHY-8114611.

References

- [1] R.A. Copeland and D.R. Crosley, *Chem. Phys. Letters* 107 (1984) 295;
R.A. Copeland, M.J. Dyer and D.R. Crosley, *J. Chem. Phys.* 82 (1985) 4022.
- [2] R.K. Lengel and D.R. Crosley, *Chem. Phys. Letters* 32 (1975) 261; *J. Chem. Phys.* 68 (1978) 5309.
- [3] R.A. Copeland, M.L. Wise and D.R. Crosley, *J. Phys. Chem.* (1988), to be published.
- [4] P.W. Fairchild, G.P. Smith and D.R. Crosley, *J. Chem. Phys.* 79 (1983) 1795.
- [5] R.A. Copeland and D.R. Crosley, *J. Chem. Phys.* 84 (1986) 3099;
J.B. Jeffries, R.A. Copeland and D.R. Crosley, *J. Chem. Phys.* 85 (1986) 1898;
G.P. Smith and D.R. Crosley, *J. Chem. Phys.* 85 (1986) 3896.
- [6] C.B. Cleveland and J.R. Wiesenfeld, *Chem. Phys. Letters* 144 (1988) 479.
- [7] A. Hofzumahaus and F. Stuhl, *J. Chem. Phys.* 82 (1985) 3152;
N.L. Garland and D.R. Crosley, in preparation.
- [8] R.A. Copeland, M.L. Wise, K.J. Rensberger and D.R. Crosley, in preparation.
- [9] N.L. Garland, J.B. Jeffries, D.R. Crosley, G.P. Smith and R.A. Copeland, *J. Chem. Phys.* 84 (1986) 4970.
- [10] N.L. Garland and D.R. Crosley, *Twenty-First Symposium (International) on Combustion (The Combustion Institute, Pittsburgh, 1988)* p. 1693.
- [11] I.S. McDermid and J.B. Laudenslager, *J. Chem. Phys.* 76 (1982) 1824.
- [12] K.J. Rensberger, M.J. Dyer and R.A. Copeland, *Appl. Opt.* (1988), to be published.
- [13] K.J. Rensberger, J.B. Jeffries, R.A. Copeland, K. Kohse-Höinghaus, M.L. Wise and D.R. Crosley, in preparation.
- [14] K.H. Eberius, K. Hoyermann and H.Gg. Wagner, *Thirteenth Symposium (International) on Combustion (The Combustion Institute, Pittsburgh, 1971)* p. 713.
- [15] J. Brzozowski, P. Erman and M. Lyra, *Physica Scripta* 17 (1978) 507;
C.W. Bauschlicher Jr. and S.R. Langhoff, *J. Chem. Phys.* 87 (1987) 4665.
- [16] P.M. Doherty and D.R. Crosley, *Appl. Opt.* 23 (1984) 713.
- [17] D. Stepowski and M.J. Cottreau, *J. Chem. Phys.* 74 (1981) 6674;
R.P. Lucht, D.W. Swecny and N.M. Laurendeau, *Appl. Opt.* 25 (1986) 4086.
- [18] R.A. Kee, J.F. Grcar, M.D. Smooke and J.A. Miller, *Sandia National Laboratory Report, SAND85-8240* (1985).
- [19] R.A. Kee, J.A. Miller and T.A. Jefferson, *Sandia National Laboratory Report, SAND80-8003* (1980).
- [20] G.P. Smith, *Chemical Mechanics for Modeling Low-Pressure H₂-N₂O-O₂ Flames*, SRI Report MP 88-006 (1988).
- [21] J. Warnatz, in: *Combustion chemistry*, ed. W.C. Gardiner Jr. (Springer, Berlin, 1984) ch. 5.
- [22] R.K. Hanson and S. Salimian, in: *Combustion chemistry*, ed. W.C. Gardiner Jr. (Springer, Berlin, 1984) ch. 6.
- [23] P. Marshall, A. Fontijn and C.F. Melius, *J. Chem. Phys.* 86 (1987) 5540.
- [24] K. Kohse-Höinghaus, J.B. Jeffries, R.A. Copeland, G.P. Smith and D.R. Crosley, *Twenty-Second Symposium (International) on Combustion (The Combustion Institute, Pittsburgh, 1989)*, to be published.
- [25] P. Papagiannakopoulos and C. Fotakis, *J. Phys. Chem.* 89 (1985) 3439.
- [26] K.H. Becker, D. Haaks and T. Tatarczyk, *Chem. Phys. Letters* 25 (1974) 564.